Resolution on multiples: Interpreters' perceptions, decision making, and multiple attenuation

Lee Hunt, Scott Reynolds, Mark Hadley, and Scott Hadley, Fairborne Energy, Ltd.
Ye Zheng, Divestco Inc.
Mike Perz, Arcis Corporation

We investigated our ability to remove a specific short-period multiple from the Nisku and Blueridge formations in West Central Alberta, Canada. This problem is commercial in nature, and has persisted because it was believed that the multiple had too little moveout to be removed, rendering interpretation of the thin Blueridge zone impossible. Associated with this issue was the belief that the modern high-resolution Radon transforms do not materially affect the stack response of real data in this area despite their excellent performance on synthetics and on other data in the literature. Serious technical work seldom affords a discussion of "beliefs", but this work is concerned with the decision-making of the interpreter. We show that in order to address a specific, real, short-period multiple problem, the interpreter was required to challenge previously held technical assumptions. This required the interpreter to consider the nature of the multiple itself, the nature and limitations of the multiple suppression technology used, and to objectively measure the level of success in suppressing the multiple.

The first steps in this process were to confirm the existence of the short-period multiple, and to identify the probable multiple generators as well as the approximate minimum differential moveout of the multiple. This analysis suggested that the differential moveout was as little as 12 ms at the far offset of 4000 m. This knowledge motivated us to consider a practical strategy aimed at achieving a Radon transform with the optimal resolution and behavior. Our strategy involved minimizing both inaccuracies and spread in the Radon transform caused by smearing of geology, lateral velocity changes, noise, poor sampling in the land 3D, and a low-bandwidth wavelet. The noise and poor sampling were major concerns that we felt could be dealt with by employing a 5D interpolation prior to multiple attenuation rather than using common-offset stacking or borrowing procedures. The idea was to avoid potential structural smearing that might arise from less sophisticated methods of handling the noisy, poorly sampled gathers. The 5D interpolation was included in a high-resolution and AVO-compliant processing flow. This new processing flow allowed us to improve the performance of the Radon transform and apply a very aggressive filter in tau-p space. We measured the quality of the stack results by correlation with a synthetic seismogram and compared the correlations to the results produced by other preprocessing flows, including ones without interpolation and with different tau-p mutes. We found that our aggressive multiple attenuation was beneficial to the stack results, and that the interpolation led to better stacks and better behaved tau-p spaces. The correlation results with the various processing flows illustrate that the stack response did improve; it improved the most with an aggressive multiple attenuation, and with the interpolation flow. The correlations also show that velocity analysis and wavelet resolution are important. This work thus demonstrates the importance of the entire processing flow in achieving optimal multiple suppression and quality well ties. We show that the interpolation-high resolution Radon transform flow was superior because of its effect on the signal-to-noise ratio of the data input to the transform as well as its minimization of geologic smearing. The concept of the interpreter's technical assumptions (or beliefs) is undeniably tied to the value of this work. The aggressive tau-p mute could only be chosen be-

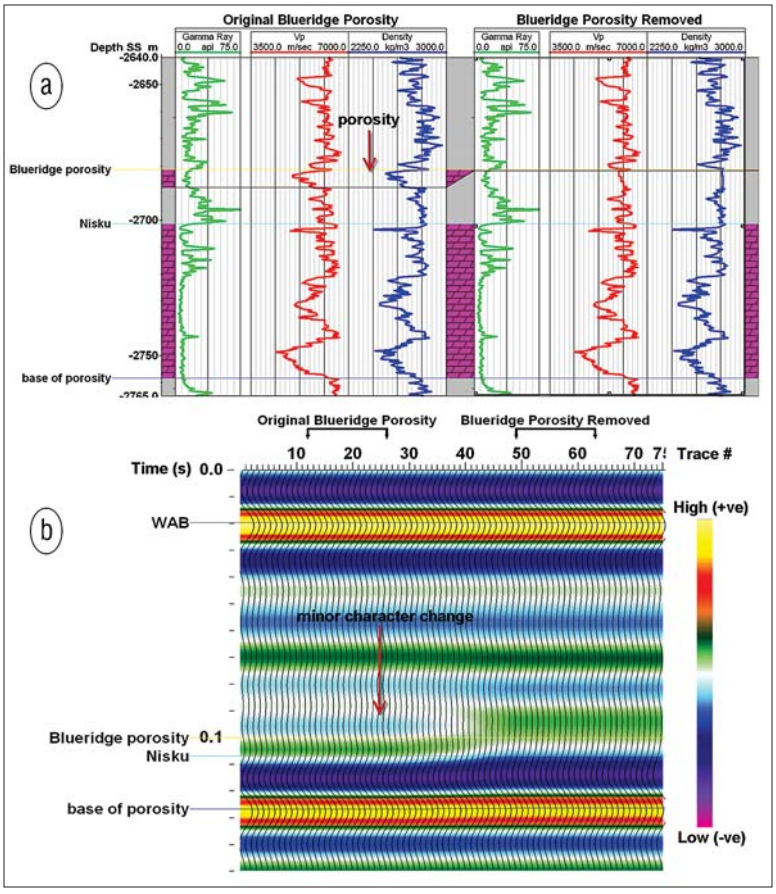

Figure 1. *The Nisku and Blueridge formations as represented by a deep well that ties near the center of the survey. (a) The stratigraphy with and without Blueridge porosity. (b) A simple normal-incidence seismic model. Changes in amplitude associated with the Blueridge porosity are visible but minor.*

cause we identified the multiple generators and estimated the expected differential moveout of the multiple. Without this prior knowledge, it is extremely unlikely that any interpreter would choose to apply such an aggressive tau-*p* mute. We will discuss the effect of these efforts on the decision making of the interpreter further, including the importance of the quality as well as the resolution of the tau-*p* space.

The Nisku and Blueridge formations

The Nisku Formation in the Deep Basin area commonly consists of thick reefal carbonate that grows on the Bigoray/Lobstick platform. The reefs can have a thickness up to 75 m and porosities over 10%. The equivalent off-reef material consists of tight, fine-grained, open marine carbonates. The Blueridge carbonate overlays the Nisku, but is not pervasive. The Blueridge can produce at economic rates over significant areas, and is an attractive target in the area. Blueridge reservoir locally develops in dolomitized grainstone shoals, which may or may not be related to the underlying Nisku reefal development. The Blueridge reservoir commonly has a thickness of less than 8 m and can have porosities approaching 10% locally. The Blueridge reservoir is challenging to image because it is thin and affected by the more dominant Nisku reef response. Figure 1 depicts the Nisku and Blueridge stratigraphy using a deep well that ties near the center of the 3D survey. The Blueridge porosity is completely removed on the right half of the model, which is equivalent to off-shoal, tight, material. The amplitudes at the Blueridge level are low, and the variations due to the change in porosity are minor but visible.

As Figure 1 indicates, delineation of the Blueridge reservoir is expected to be challenging due to the small amplitude variations observed from modeled changes in reservoir quality. Figure 2 shows the original (legacy) processed seismic line from a 3D survey. This line goes through a well that encountered Blueridge porosity and a thick Nisku reef. The amplitudes at the Blueridge level are clearly much too high, and are thought to be an indication of multiple contamination.

The prevailing opinion regarding the Blueridge zone was that it was not possible to map it or explore for it as a primary target. The subtlety of its expected seismic response from modeling (as in Figure 1) combined with the poor tie to well control (as in Figure 2) were considered too difficult to overcome. Short-period multiple contamination was blamed for the poor tie. Earlier attempts at multiple attenuation with the Radon transform were reported as failures. In fact, the advice was that this problem could not be solved with the Radon transform. We felt that the old assessment was prejudicial, and should be examined critically. The economic value of the resource warranted a new look.

Multiples and the high-resolution Radon transform

The earliest and longest-standing approach to attacking multiples has been through exploiting their velocity characteristics. Dix (1955) suggested that multiples could be identified because they would have "absurd" velocities. These velocities would be slower than the trend of primaries and thus yield small or even negative interval velocities. This assessment was a necessary consequence of the assumption that interval velocities generally increase with increasing depth. Mayne's (1962) development of the common-midpoint (CMP) method enabled the creation of localized velocity spectra (Taner and Koehler, 1969) in which primaries and multiples could be observed. These spectra employed stacking or similarity measures along hyperbolic trajectories as defined by Dix, whose work could also be used to estimate the velocity of each interval, and his equations related to velocity are still used today.

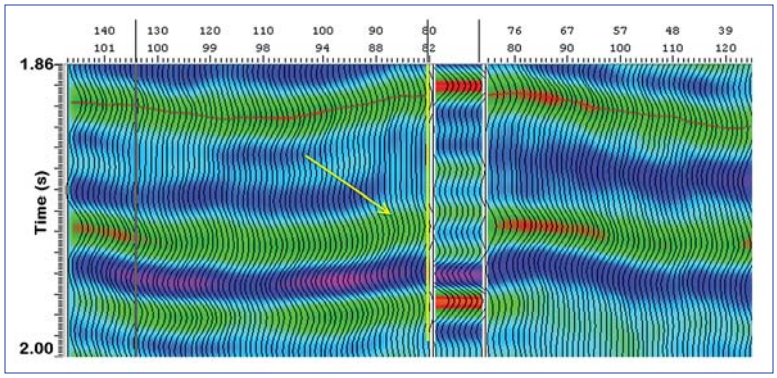

Figure 2. *Original (legacy) seismic line through a Nisku reef and Blueridge porosity. The yellow arrow depicts the well tie, synthetic, and Blueridge zone. The thin red horizon line depicts the Wabamun top. The amplitudes at the Blueridge level (red) are much higher than expected (blue and green) from the synthetic tie.*

The Radon transform is a popular and intuitive method for the attenuation of multiples because it exploits the difference in rms velocity, or moveout, of the multiples relative to the primaries. It does this by representing the data much like a velocity spectra. The Radon transform typically uses parabolas or hyperbolas as its basis function when used for multiple attenuation. In either case, the CMP time-offset data are represented by data ordered in intercept time, tau (T) and the curve parameter, *p*. If hyperbolic basis functions are used, *p* represents slowness, and tau-*p* space is essentially a velocity stack (Thorson and Claerbout, 1985). Early implementations by Thorson and Claerbout and Hampson (1986) both solved the Radon transform based on the following underdetermined system of equations $Lm = d$ (d = the data, m = the data model weights in the Radon domain, and L = the basis function operator). Both approaches combat nonuniqueness through the use of constraints, with the former method using sparsity constraints while the latter using nonsparse constraints. Sacchi and Ulrych (1995) emphasized that this solution was nonunique and poorly resolved due to limitations in all surface seismic experiments, and they proposed computationally efficient sparsity constraints to mitigate these problems. These sparsity constraints have a physical interpretation that is related to the data aperture: the near- and far-offset limitations represent missing data or truncations of the CMP gathers. These artifacts are minimized by the sparsity. In effect, the sparsity can be thought

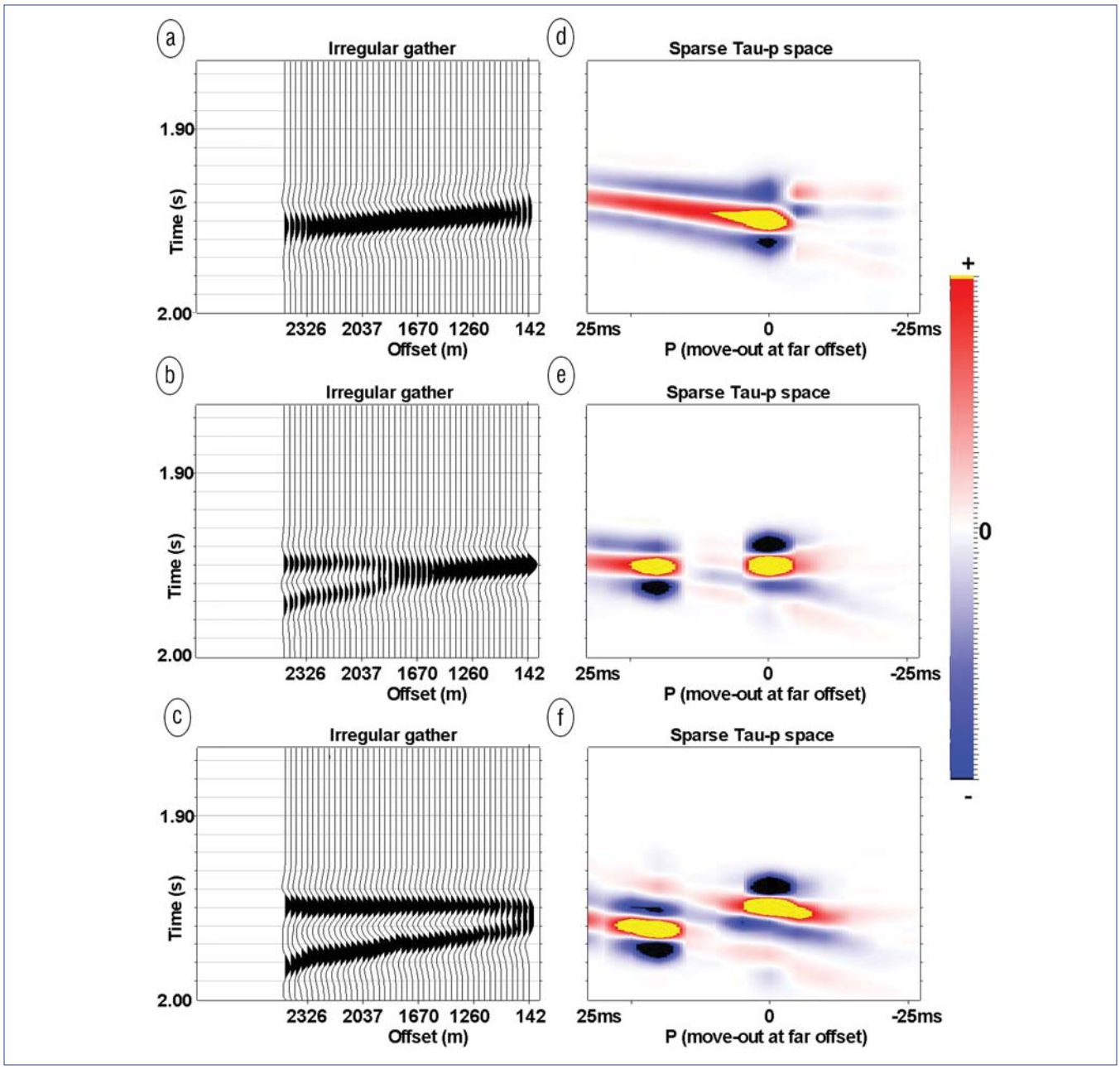

Figure 3. *A multiple with 20 ms of differential moveout relative to the primary event at 2500 m was generated. Each event has the same amplitude, and a 35-Hz Ricker wavelet was used. The intercept time, tau, of the multiple is varied in this figure. (a) The intercept of the multiple is 10 ms above the primary. (b) Both events start at the same time. (c) The intercept of the multiple is 10 ms below the primary. The tau-*p *spaces for (a), (b), and (c) are given in (d), (e), and (f), respectively. Despite using a sparse Radon algorithm, the events do not separate completely in the tau-*p *space of (d).*

of as extending the aperture infinitely and thus reducing the "bow-tie" operator artifacts in tau-*p* space (Sacchi and Ulrych). Cary (1998), Ng and Perz (2004), and others developed this idea commercially and implemented it for both parabolic and hyperbolic applications that could be solved in either the time or frequency domain (Sacchi, 2009). The use of sparsity constraints is now common in high-resolution Radon transforms, and these modern transforms are widely accepted as superior to previous moveout-based methods, especially when supplemented with interactive graphical tools for time- and space-variant Radon mute definition.

Limitations or risks of the Radon transform

Despite the fact that we use a sparse Radon transform, smearing persists to some degree in the tau-*p* spaces of real seismic data. This means that we cannot always know whether or not we can safely remove a multiple with very small differential moveout. The problem involves two things: the ability to identify the multiple in tau-*p* space, and the ability to safely remove it. Both identification and safe removal require that the primary and multiple be fully separated in tau-*p* space, which is inextricably related to how focused the events are in that space. Real data differ from simple constant amplitude

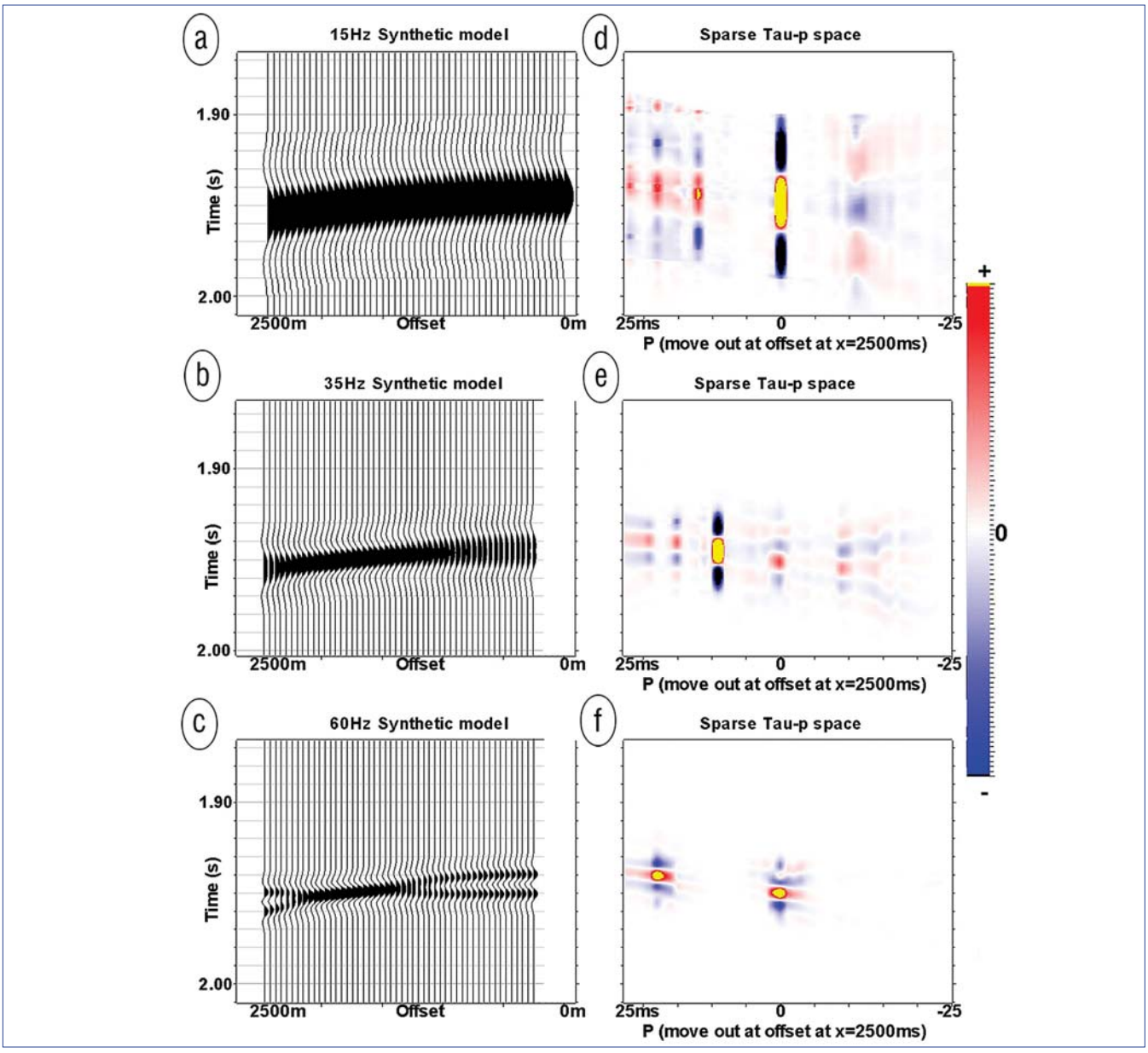

Figure 4. *The effects of wavelet resolution in the resolution of the Radon transform. The offset bins are also perfectly regular, with 50-m spacing. (a), (b), and (c) depict a flat primary and a multiple. In each case, the multiple starts 10 ms above the primary, and has a differential moveout of 20 ms at 2500 m. We used Ricker wavelets with dominant frequencies of 15 Hz, 35 Hz, and 60 Hz in (a), (b), and (c), respectively. (d), (e), and (f) represent the tau-*p *spaces for (a), (b), (c), respectively. The low-resolution gather of (a) yields an inaccurate and unresolved tau-*p *space in (d). This problem is incorrect in a different way with the wavelet used in the gather of (b), and the corresponding tau-*p *space shown in (e). The problem is only completely resolved with the highest-frequency wavelet of (c) and the tau-*p *space of (f).*

synthetic events in numerous ways which affect resolution in Radon space. To understand this disappointing fact, we must consider firstly that however sparse the transform is supposed to be, it must still reconstruct the original CMP gather, and secondly how easily that the data can be represented by the basis functions. This has several implications:

1) Amplitude variations with offset in the data will cause smearing and lack of resolution in tau-*p* space. The problem was discussed by Thorson and Claerbout, Kabir and Marfurt (1999), and Verschuur (2007). Ng and Perz's model work showed that a sufficiently large AVO response on a single event could actually appear to be two separate and smeared events. This implies that it is possible to destroy AVO characteristics in the data by applying a Radon-domain mute between two events that are mistakenly interpreted as a primary and a multiple (when in fact, they represent one event which has AVO). This is a serious risk if very aggressive multiple attenuation is contemplated.
2) Separation of closely spaced events, with similar moveout in tau-*p* space, requires that the character of the data across the input CMP is actually indicative of two events. It has

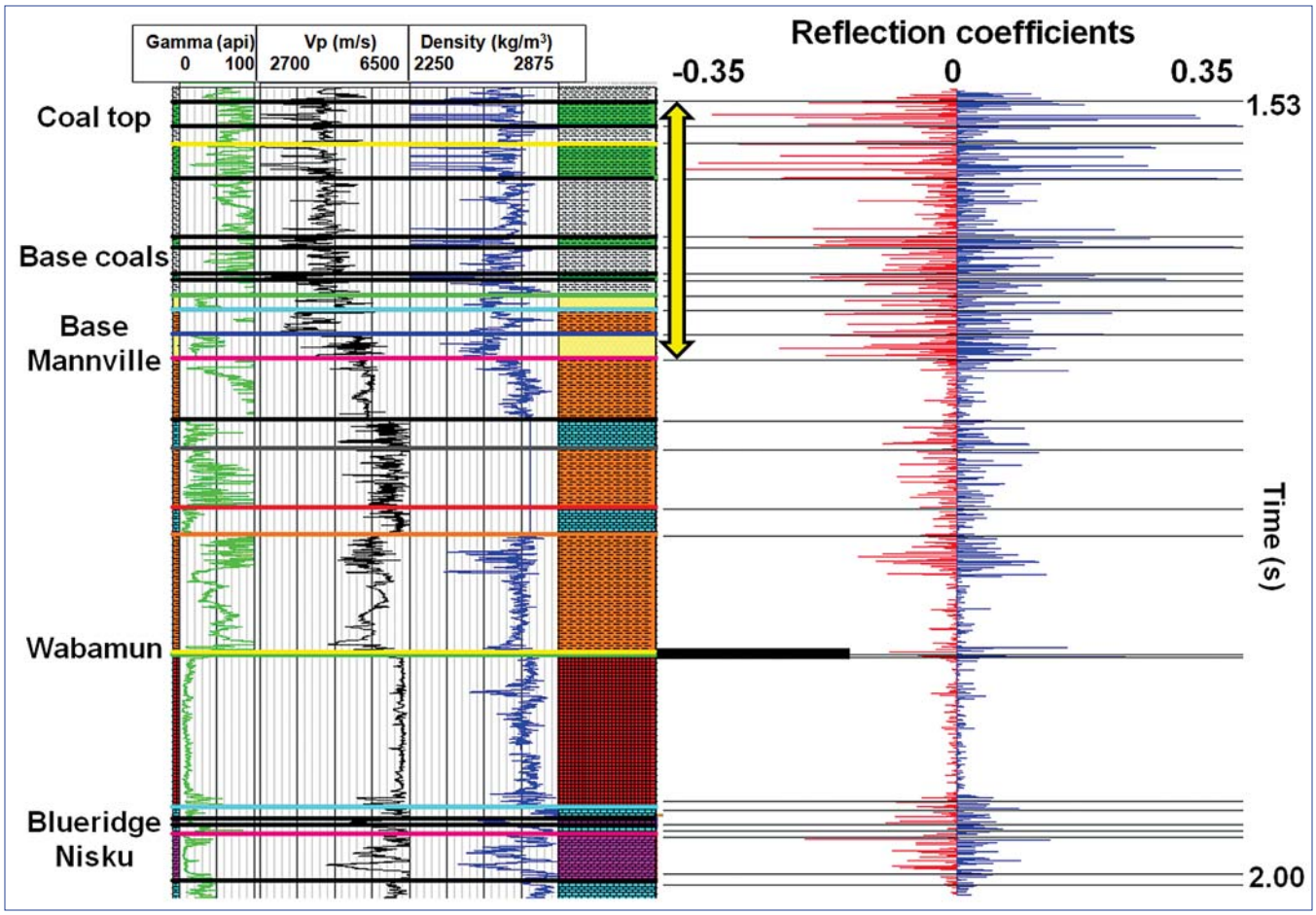

Figure 5. *The velocity structure of the area is represented by the sonic log of the deep well discussed earlier. The velocity profile increases materially at the Wabamun level. The Blueridge and Nisku lie below a thick, high-velocity section with no strong reflections. For a multiple to have an intercept near the Blueridge, it must either bounce numerous times or it must peg-leg off the Wabamun event. The yellow arrow indicates the coal section within which the reverberations will be generated before peg-legging off the Wabamun.*

two clear implications: first that the way in which the primaries and multiples interfere can be important, and secondly that the size of the wavelet in the data can also be important. Although typical synthetics demonstrating the resolution of the sparse Radon transform illustrate the separation of each event in tau-*p* space quite well, the effect of different interference patterns for the same differential moveout has not been thoroughly discussed. Figure 3 illustrates a primary and multiple with the same amplitudes. The differential moveout of the multiple with respect to the primary is 20 ms at 2500 m offset. The intercept time, tau, of the multiple is varied and the offsets were taken from a typical CMP from the 3D to simulate land 3D irregularity. A 35-Hz Ricker wavelet was used for each element of this figure. In Figure 3a, the multiple starts 10 ms above the primary. In Figure 3b, both events start at the same time and, in Figure 3c, the intercept of the multiple is 10 ms below the primary. Only a very narrow range of Radon space is shown in the corresponding tau-*p* spaces of Figures 3d, 3e, and 3f, which makes this an unusually zoomed-in analysis. The primary and multiple are not resolved equally between these three cases, despite the fact that the differential moveout is the same. The primary and multiple events are well resolved in the tau-*p* spaces of Figure 3e and 3f but are not resolved at all in Figure 3d. The greater the interference in time and space, the more difficult it is for the sparse Radon transform to separate events correctly. This observation means we should be concerned not only with differential moveout of events, but also their relative temporal positioning.

Let us examine the effect of changes in wavelet size on the ability of the sparse Radon transform to separate multiples and primaries properly. The simple model of Figure 4 illustrates this effect. A primary and multiple are depicted in Figures 4a, 4b, and 4c. In each case, the multiple starts 10 ms above the primary and has a differential moveout of 20 ms at 2500 m. The primary and the multiple have equal amplitude and the offset bins are perfectly regular. The only differences in these three images are that the wavelet of the data changes from a 15-Hz Ricker in Figure 4a to a 35-Hz Ricker in Figure 4b, to a 60-Hz Ricker in Figure 4c. Figures 4d, 4e, and 4f represent the tau-*p* spaces for Figures 4a, 4b, 4c, respectively. The tau-*p* space corresponding to the low-resolution gather of Figure 4d clearly does not resolve the primary or the multiple; most of the energy is on the zero moveout curvature. The mid-resolution gather

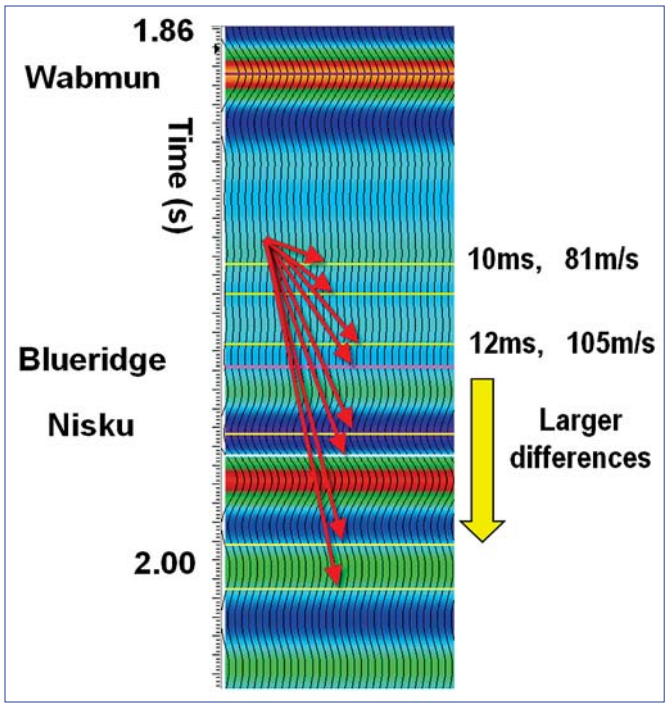

Figure 6. *A portion of the normal-incidence model of the zone of interest from Figure 1 with the calculated intercept times of the multiples indicated by the horizontal colored lines. The Blueridge and Nisku are indicated by labels only. The red arrows also point out the intercept times of these hypothetical multiples. The differential moveout and differences in rms velocity are indicated beside two of the uppermost events. The yellow arrow indicates that interfering multiples with later arrivals have higher differential moveouts. This indicates that the smallest differential moveout we have to be concerned with is 12 ms.*

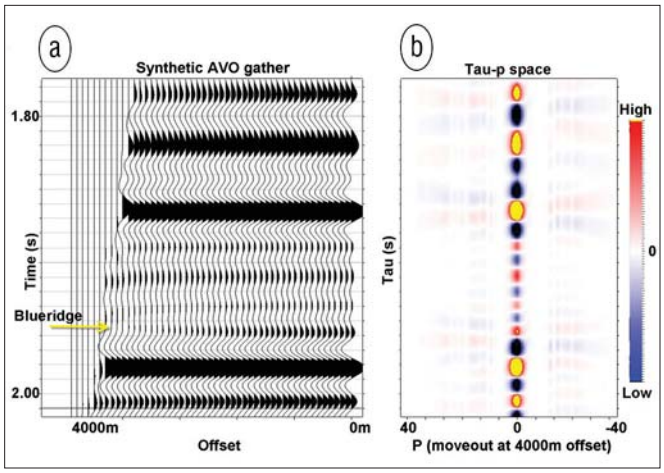

Figure 7. *Shuey (1985) estimate of AVO at the Blueridge level. (a) Shuey model gather for the Blueridge. It exhibits small AVO affects. The data are muted at 30°. (b) The forward Radon space of this model. The tau-p image is well resolved, indicating that the small amount of AVO at our zone of interest does not cause serious spread in Radon space.*

fares little better: Figure 4e shows the energy is misallocated in quantity and position. Only the highest-resolution gather of Figure 4c and its tau-*p* space of Figure 4f does a perfect job of resolving both events, and correctly representing the moveout of each event. These resolution issues will vary depending on the intercept (tau) of each event, and the exact way in which the events interfere in time and offset as depicted in Figure 3. By comparing Figure 4b and Figure 3, we also see that the worst case scenario for resolving multiples and primaries involves a multiple that superimposes symmetrically over the primary, which is the case for Figure 4. Given these issues, we must be wary that the transform may not always uniquely and correctly separate events in tau-*p* space, despite its sparseness. Our best practical action is to increase the resolution of the wavelet as much as possible. The greater the wavelet resolution, the greater our ability to accurately separate events.

3) The events must actually be hyperbolic (or parabolic, if the basis functions are parabolic) in nature. Dips or lateral variations in the velocity field could potentially create departures from the basis function that would in turn limit resolution (Dix; Sherwood, 1972; and Verschuur, 2006).
4) Sherwood noted that CMP gathers were noisy, leading him to suggest the use of several CMP gathers in velocity analysis. Neighboring CMPs can be interleaved to form one larger "supergather" and optionally, all supergather data can be stacked into predefined, regular, offset bins to form a common-offset gather, or COFF. The use of too many CMP gathers over too large an area in either scheme may reduce noise, but could limit Radon-domain resolution by virtue of problem 3 above. Any change in structure, wavelet, dip, or velocity over the gathered area will cause some smearing.
5) Missing offsets, particularly near offsets, cause smearing in tau-*p* space. The familiar bow-tie effect is caused by the near- and far-offset truncation, but additional events in tau-*p* space can be created by offsets missing anywhere in between. Marfurt et al. (1996) illustrated this in detail; however, the sparse Radon transform has been shown to be effective at combating this problem (Sacchi and Ulrych). Despite this, there are still minor advantages to be gained from using regular offsets with the sparse Radon transform. We can see that events in the tau-*p* space of Figure 3d may be slightly less resolved than in Figure 4e. These two sets of figures have identical wavelets and identical events, but Figure 3 has irregular offsets, versus the perfectly regular offsets of Figure 4. On this extremely zoomed-in observation of tau-p space, the evidence suggests regularity still retains some desirability. Therefore, in land 3D, concerns for missing offsets have likely contributed to the legacy habit of forming supergathers or COFFs prior to application of the Radon transform.

Strategy to achieve the highest-quality Radon transform on land 3D data

In order to have the highest-resolution Radon transform and most effective multiple attenuation possible, we devised a strategy to mitigate the limitations described above. We felt it was important that this strategy be practical so that any interpreter could use a similar approach. Therefore, only simple modeling was used rather than specialized tools. This strategy involved five elements:

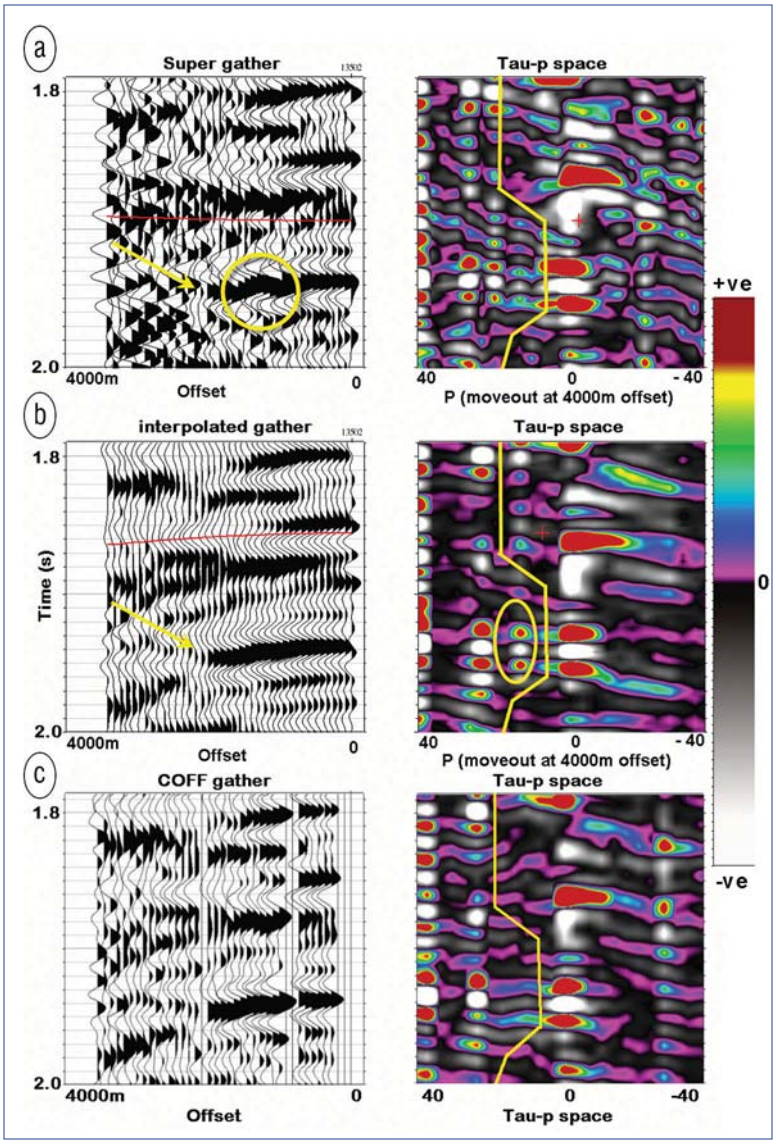

Figure 8. *Gather and tau-*p *space (respectively) from (a) the sparse Radon transform with super-binning, (b) sparse Radon transform with 5D interpolation, and (c) sparse Radon transform of a 3 × 3 COFF stacked gather. The Blueridge level is identified with a yellow arrow. The harsh mute is in yellow. The worst case multiple (predicted to have about 12 ms of differential moveout) is only resolved in the interpolated gather of (b) where it is circled.*

Understanding the multiple

There are many multiples in the data, but they are not all of equal concern to us. In order to understand the specific problem at hand, we investigated the velocity structure of the area. Figure 5 illustrates the velocity profile and reflection coefficients for the deep well. The sonic velocity increases with depth, profoundly so at the Wabamun level. The Blueridge and Nisku lie below the Wabamun and below a thick section with no strong reflections. This velocity structure makes several things apparent. The high velocity of the Wabamun section means that most multiples will have significantly different rms velocities and differential moveouts than the Blueridge and Nisku reflections. The later multiple arrivals will generally have larger differences. We are only concerned with the small differential-moveout multiples, so this observation removes most multiples from our consideration. Multiples with more than one extra reverberation are mostly removed from consideration because either they will have smaller amplitudes, or the material they travel through is necessarily so slow that they have large differential moveout. Surface-related multiples would also have too much differential moveout to be considered. By following this logic, we concluded that the multiples of greatest concern were likely peg-leg multiples that reverberated once in the coal section, and then peg-leg off the Wabamun.

In order to estimate the differential moveout of the relevant multiples, we created simple models of the proposed peg-leg pathways and calculated their rms velocities and intercept times with the model data and Dix's equations. We used the P-wave velocity data from the sonic log and modeled traveltimes and rms velocities for possible multiples involving the coals, the base of the Mannville section, all peg-legging off the Wabamun marker. Figure 6 illustrates the results of this modeling and associated calculations on a portion of the normal-incidence model from Figure 1. The intercept times of the calculated multiples are indicated by horizontal colored lines. The differential moveout and difference in rms velocity between the primary and multiple events is indicated at two of the early intercept times. The multiples that arrive later will have larger differences in rms velocity and differential moveout. These calculations indicate that the most difficult multiple to remove will have a differential moveout of about 12 ms at 4000 m. This would require a very tight mute in tau-*p* space, and is concerning.

1) Understanding the multiple of interest so we know where to expect its location in tau-*p* space. This is somewhat driven by our concerns of mistakenly filtering out an AVO response.
2) Checking if a significant AVO response should be expected at the zone of interest, and estimating if that AVO response would cause significant spreading in tau-*p* space.
3) Ensuring that the velocity picking on the 3D survey was consistent with the known velocity structure of the area as well as the horizons themselves.
4) Reducing the need to supergather or stack CMPs prior to applying the Radon transform.
5) Increasing the temporal resolution and signal-to-noise ratio of the data as much as possible.

Can we preserve the AVO in the data?

The potential effect of AVO in the data was most easily addressed through simple forward modeling. We created a simple Shuey (1985) AVO model using the deep well tie. This model used offsets to 30°, which was equivalent to both the

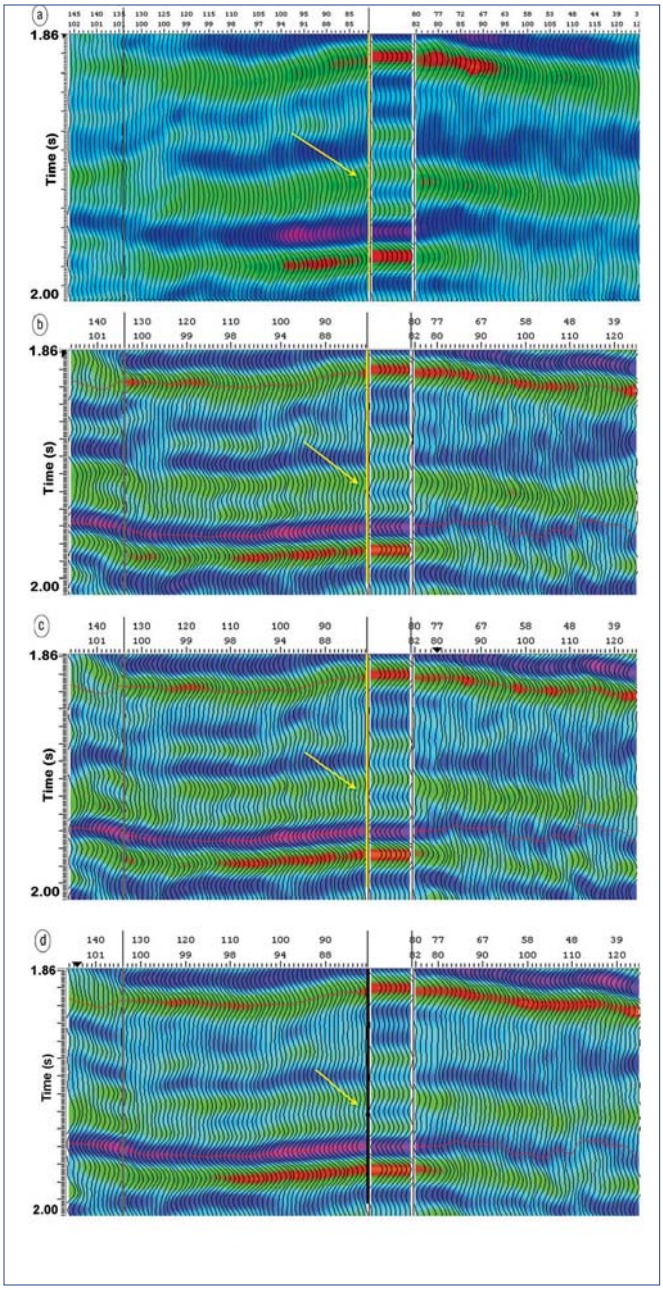

Figure 9. *Reprocessing results: (a) optimal new velocities, (b) reprocessing including optimized velocities, noise attenuation, and spectral balance, but no interpolation, (c) the full reprocessing but no interpolation, and sparse Radon transform with the mild mute, and (d) the full reprocessing as well as 5D interpolation, and sparse Radon transform with the aggressive mute. These four comparison stacks are also identified in Table 1 by the bold text. These stacks are all improvements over the legacy stack of Figure 2 and (d) has the best overall match.*

offset and angles found in the actual 3D data. This model is illustrated in Figure 7. Figure 7a shows the gather itself, which has some minor AVO characteristics in the Blueridge. We performed the high-resolution Radon transform on this gather and illustrate the tau-*p* space in Figure 7b. The velocity space image does not suffer significant smear due to the AVO. This simple model indicates that the primary should be well resolved in tau-*p* space, and that we may be able to safely perform aggressive filtering close to the moveout of the primary.

Multi-CMP gathering versus multidimensional interpolation

Land 3D seismic data are typically noisy and poorly sampled. As mentioned earlier, supergather CMPs and offset binning can improve the sampling and signal-to-noise characteristics of gathers used in the Radon transform. Despite the fact that the sparse Radon transform is less affected by sampling, these methods are still employed, presumably to reduce noise in the gathers. We propose that 5D interpolation (Liu and Sacchi, 2004; Sacchi and Liu, 2005; Trad, 2007) may be a better way to regularize the data prior to the Radon transform since it has been shown (Hunt et al., 2010) to introduce less geological smear than superbinning. Interpolation should also tend to reduce overall noise level, since the number of traces increases, and many noise types do not interpolate as well as signal. Combining interpolation with the sparse Radon transform should produce tau-*p* spaces with the greatest resolution in the transform domain.

Velocities and resolution: The processing flow

We employed an aggressive AVO-compliant processing flow that was aimed to achieve stable, high-resolution data. Our processing flow included these key steps:

- Horizon-based velocity analysis. The horizons were picked by the interpreter so that NMO corrections could be consistently picked. The well-log-derived interval velocities were also used as a guide. These two controls ensured that the velocities were picked in a geologically consistent manner.
- Cascaded surface-consistent deconvolution and surface consistent prestack *f-x* noise attenuation (Wang, 1996) were applied.
- 5D interpolation (Trad, 2007) was applied to reduce the need to borrow traces in multiple modeling and to reduce noise in the gathers.
- Aggressive and mild multiple attenuation were employed according to our expectations of the moveout of the multiple.
- Spectral balancing was applied to the stack data.

Method

The data were stacked at each of the key processing steps, resulting in ten different seismic volumes for comparison (Table 1). All results are improvements over the legacy processing result of Figure 2. The comparison also isolates the method of regularization by comparing super gathering against interpolation. The tau-*p* mutes are picked in two ways: a mild mute picked on the tau-*p* space of superbinned gathers, and a more aggressive mute picked on the tau-*p* space calculated from interpolated gathers. We also captured images of the tau-*p* spaces of some of these different approaches for comparison. We used simple correlation with our well tie to quantitatively evaluate the quality of the results. The well

Starting point	Regularization	Radon transform	Tau-*p* mute	CC-big window	CC-small window	Key difference	Improvement
Original (legacy) processing	None	None	None	0.654	0.614	Velocities	0%
Optimal (new) velocites	**None**	**None**	**None**	**0.723**	**0.635**		**3%**
Final noise-attenuated gathers, no spectral balance	Superbinning	None	None	0.774	0.729	Velocities + best noise attenuation	19%
Final noise-attenuated gathers, no spectral balance	Interpolation	None	None	0.789	0.729		19%
Final noise-attenuated gathers, has spectral balance	**None**	**None**	**None**	**0.811**	**0.769**	Add spectral balance	**25%**
Final noise-attenuated gathers, has spectral balance	Interpolation	None	None	0.816	0.788		28%
Final noise-attenuated gathers, has spectral balance	**Superbinning**	**Sparse Radon transform**	**Mild mute**	**0.844**	**0.848**	Radon transform	**38%**
Final noise-attenuated gathers, has spectral balance	Superbinning	Sparse Radon transform	Aggressive mute	0.869	0.876		43%
Final noise-attenuated gathers, has spectral balance	Interpolation	Sparse Radon transform	Mild mute	0.847	0.859	5D interpolation + Radon	40%
Final noise-attenuated gathers	**Interpolation**	**Sparse Radon transform**	**Aggressive mute**	**0.883**	**0.924**		**50%**

Table 1. *Summary of the experiment with cross-correlation values with the well tie. The "CC" columns give the correlation coefficient of the larger and smaller windows. The interpolation plus multiple-attenuation flow yielded the best correlation coefficients. The four example stacks shown in Figure 9 are bolded for clarity. The improvement given is the relative improvement versus the reference original stack of Figure 2.*

log was correlated with each data volume identically using a small window around the Nisku and Blueridge (1900–1992 ms), and a larger correlation window (1860–1992 ms). Each correlation was also perturbed with ten minor static shift plus correlation jiggles to ensure that the correlation coefficients were determined as fairly as possible. This method allows us to evaluate our results by observing the stacks, the gathers and tau-*p* spaces, and by comparing the correlation coefficients with the synthetic.

Results

Figure 8 shows production gathers and forward Radon transforms (tau-*p* spaces) at one CMP location for the supergathered sparse Radon transform and the sparse Radon transform with 5D interpolation. We also included a gather created by a 3 × 3 COFF stacking of all data centered on the CMP. The 5D interpolated example of Figure 8b is more resolved at the Blueridge level, and illustrates a multiple with 12 ms of moveout, which we expected. The tau-*p* mute, shown in yellow on the right, consists of a mild mute at 22 ms of moveout at all times, and a harsh mute which cuts inside the 12-ms multiple in the zone of interest, but varies "surgically" in time. This aggressive tau-*p* mute could only be designed in the 5D interpolated tau-*p* space. The multiple identified at 12 ms in Figure 8b has limited energy, which suggests it should not dominate the stack, and therefore this multiple is unlikely to be the only reason for the poor data tie of Figure 2. We also noted the existence of this multiple with these general characteristics in numerous other gather comparisons elsewhere across the survey.

Figure 8 illustrates two differences in the data gathers: first, the 5D interpolated gather and the 3 × 3 COFF stacked gather have a higher signal-to-noise ratio than the supergather and, second, the data characteristics are sensitive to these processing choices. The 5D interpolated gather appears to have retained the geologic information in the data while reducing the noise, whereas the 3 × 3 stacked gather is smeared in tau-*p* space, possibly due to velocity distortions from the gathering process. These differences are consistent with our expectations. The 5D interpolated gathers attain a higher signal-to-noise ratio because noise is reduced through the 5D interpolation, and stacking the higher-fold interpolated gathers reduces random noise. The parsimonious approach to supergathering of Figure 8a is also a disadvantage; it has not obviously smeared geologic data, but it is too noisy to yield well-resolved, interpretable tau-*p* spaces. This example illustrates that the superior appearance of the tau-*p* space of the 5D interpolated data.

Multiple attenuation was performed using these mutes. Figure 9 shows the comparison of our legacy stack (Figure 2)

and selected stacks, including the 5D interpolated plus sparse Radon transform multiple attenuation using the harsh mute. The stack response at the Blueridge level changes significantly in each case when compared to the legacy product of Figure 2, with the aggressively multiple-attenuated version of Figure 9d matching the model result of Figure 1 most closely. Contrary to the statement that "stacks do not change", the stack changes significantly in every case relative to the well tie. Moreover, although the multiple attenuated result was the best; our reprocessing for resolution and optimal velocities was responsible for a significant amount of the improvements. This is illustrated by comparing Figure 9b to Figure 2.

Correlation coefficients were calculated with the (center) well tie over the zone of interest. These correlation values are summarized in Table 1. The interpolation plus harsh multiple attenuation had the best correlation regardless of whether the larger or smaller correlation widow was used. Each successive step in the processing sequence yielded a better correlation with the well. This supports our assertion that the poor correlation of the legacy processing stack was not just caused by the multiple: better resolution, random noise handling, and velocity determination were also important.

Conclusions

Aggressive reprocessing with careful velocity analysis, AVO compliant noise attenuation and temporal resolution enhancement improved the data at the Nisku and Blueridge level. The aggressive multiple attenuation also had an additional clear, and measurable affect on the stack response. In short, the sparse Radon transform did affect the stack, contrary to the bleak legacy opinion of the problem. The combination of 5D interpolation and the sparse Radon transform produced the most stable, resolved, tau-*p* space in the observed CMP gathers. Some improvement may have come because the interpolation produced gathers with the near offsets populated. These interpolated gathers were also cleaner, and had higher signal to noise partly due to an increase in fold. This increase in data quality may be a strong contributing factor in the improved appearance of the tau-*p* space of the interpolated data. These improvements allowed us to consider and apply a more aggressive mute in tau-*p*. The mute was also consistent with the differential moveout we expected from forward modeling, which provides some confidence that the results are valid. COFF stacking to create similar increases in signal to noise was not as successful in producing well resolved tau-*p* spaces. These observations suggest the interpolation is helping in two ways: a reduction in noise as well as a minimization of smearing in velocity space due to lateral variations in the geology. The biggest advantage of the 5D interpolation plus sparse Radon transform approach is that the method enables a clear interpretation and selection of mutes in tau-*p* space. The effect of these well behaved tau-*p* spaces on the decision-making capability of the interpreter is difficult to quantify but important to discuss.

This was a commercial interpretation project, with business questions regarding the Blueridge and Nisku formations associated with it. Prior to this work, the opinion was prejudiced against even attempting multiple attenuation because of the belief that the moveout of the multiples was too small to remove. We have shown that an understanding of the multiples themselves and a well resolved tau-*p* space are better scientific tools with which to evaluate whether or not multiple attenuation should be attempted than legacy assumptions. We also showed that the short-period multiple problem was not necessarily the dominant issue in the data; increasing the temporal resolution of the stack and applying geologically consistent velocities were major contributors in improving the data.

This work did not employ esoteric or specialized modeling software. This test only required standard software, simple modeling, and the will to apply the products of previous research found in the literature. Coming back to beliefs: does the discussion of "belief" or "will" belong here? Perhaps these concepts do not, and yet our technical decisions rest at least partly on these cousins of assumption. The notion of "resolution" carries several distinct meanings, and was shown to be important throughout this work. The wavelet needs to be highly resolved prior to interpolation. The Radon transform must have high resolution in the transform domain in order to enable effective interpretation and potential mitigation. The interpreter must be resolved to do the work necessary to understand the multiple problem, and resolved to attempt to suppress the multiple even if the process is aggressive enough to be risky. We have to be resolved to move the step beyond the excellent literature that illustrates improvements on synthetics, and move to real exploration problems and the unique issues that come with them. We must also be resolved to evaluate our results quantitatively so we can measure what improvements we have made and attempt to understand why we have achieved them. TLE

References

Cary, P., 1998, The simplest discrete Radon transform: 68th Annual International Meeting, SEG, Expanded Abstracts, 17, 1999–2002.

Dix, C. H., 1955, Seismic velocities from surface measurements: Geophysics, **20**, no. 1, 68–86, doi:10.1190/1.1438126.

Hampson, D., 1986, Inverse velocity stacking for multiple elimination: Canadian Journal of Exploration Geophysicists, **22**, 44–55.

Hunt, L., J. Downton, S. Reynolds, S. Hadley, D. Trad, and M. Hadley, 2010, The effect of interpolation on imaging and AVO: A Viking case study: Geophysics, **75**, no. 6, WB265–WB274, doi:10.1190/1.3475390.

Kabir, M. M. N. and K. J. Marfurt, 1999, Toward true amplitude multiple removal: The Leading Edge, **18**, no. 1, 66–73, doi:10.1190/1.1438158.

Liu, B. and M. Sacchi, 2004, Minimum weighted norm interpolation of seismic records: Geophysics, **69**, no. 6, 1560–1568, doi:10.1190/1.1836829.

Marfurt, K. J., R. J. Schneider, and M. C. Mueller, 1996, Pitfalls of using conventional and discrete Radon transforms on poorly sampled data: Geophysics, **61**, no. 5, 1467–1482, doi:10.1190/1.1444072.

Mayne, W. H., 1962, Common reflection point horizontal stacking techniques: Geophysics, **27**, no. 6, 927–938, doi:10.1190/1.1439118.

Ng, M. and M. Perz, 2004, High resolution Radon transform in the t-x domain using "intelligent" prioritization of the Gauss-Seidel estimation sequence: 74th Annual International Meeting SEG, Ex-

panded Abstracts, 2160–2163.
Sacchi, M. D., 2009, A tour of higher resolution transforms: CSEG Annual Convention, 665–668.
Sacchi, M. D. and B. Liu, 2005, Minimum weighted norm wavefield reconstruction for AVA imaging: Geophysical Prospecting, **53**, no. 6, 787–801, doi:10.1111/j.1365-2478.2005.00503.x.
Sacchi, M. D. and T. D. Ulrych, 1995, High-resolution velocity gathers and offset space reconstruction: Geophysics, **60**, no. 4, 1169–1177, doi:10.1190/1.1443845.
Sherwood, J. W. C. and P. H. Poe, 1972, Continuous velocity estimation and seismic wavelet processing: Geophysics, **37**, no. 5, 769–787, doi:10.1190/1.1440299.
Shuey, R. T., 1985, A simplification of the Zoeppritz equations: Geophysics, **50**, no. 4, 609–614, doi:10.1190/1.1441936.
Taner, M. T. and F. Koehler, 1969, Velocity spectra-digital computer derivation and applications of velocity functions: Geophysics, **34**, no. 6, 859–881, doi:10.1190/1.1440058.</
Thorson, J. R. and J. F. Claerbout, 1985, Velocity-stack and slant-stack stochastic inversion: Geophysics, **50**, no. 12, 2727–2741, doi:10.1190/1.1441893.
Trad, D., 2007, A strategy for wide-azimuth land data interpolation: 77th Annual International Meeting, SEG, Expanded Abstracts, 946–950.
Verschuur, D. J. and A. Berkhout, 2005, Removal of internal multiples with the common-focus-point (CFP) approach: Part 2—Application strategies and data examples: Geophysics, **70**, no. 3, V61–V72, doi:10.1190/1.1925754.
Verschuur, D. J., 2006, Seismic multiple removal techniques: past, present and future: EAGE Publications.
Verschuur, D. J., 2007, Expert answers: Does parabolic Radon transform multiple removal hurt amplitudes for AVO analysis? Answer 2: CSEG Recorder, **32**, 3, 10–14.
Wang, X., 1996, Surface consistent noise attenuation of seismic data in frequency domain with adaptive pre-whitening: 65 Annual International Meeting, SEG, ExpandedAbstracts, 1192–1195.

Acknowledgments: We thank Mauricio Sacchi of the University of Alberta for his advice on this project, Darren Betker and Earl Heather of Divestco for their efforts in processing, and Fairborne Energy Ltd. for allowing us to show this information.

Corresponding author: LHunt@fairborne-energy.com